Supporting information

Photochemical benzylic radical arylation promoted by supported Pd nanostructures

Teresa A. Gawargy, Paolo Costa, Anabel E. Lanterna* and Juan C. Scaiano*

Department of Chemistry and Biomolecular Sciences and Centre for Advanced Materials Research (CAMaR), University of Ottawa, 10 Marie Curie, Ottawa, Ontario K1N 6N5, Canada.

Table of Content

Experimental details

All chemicals were purchased from Sigma Aldrich and used as received unless otherwise stated. TiO_2 P25 was purchased from Univar Canada, and 1wt% Au@TiO_2 from Strem Chemicals (AUROlite™ Au/TiO_2). Metal loading on the different catalysts was determined by Inductively Coupled Plasma Optical Emission Spectrometry (ICP-OES), using an Agilent Vista Pro ICP Emission Spectrometer. Approximately 10 mg portions were accurately weighed in triplicate and digested with aqua regia. Solutions were further diluted and measured by ICP-OES. Photochemical coupling of benzyl radicals was carried out under UVA irradiation using Luzchem LZC-UVA lamps. Characterization of the coupling products was performed by mass spectrometry in an Agilent 6890-N Gas Chromatograph with an Agilent 5973 mass selective detector calibrated with acetophenone.

Catalyst characterization

The Pd@TiO_2 catalyst was synthesized as previously described.[1] Figure S1 and Table S1 summarise the properties of three different batches used for this work.

Catalyst reducing treatment

The treatment used was based on our previous report.[2] Briefly, to prepare the reduced catalyst, 200 mg of the catalyst (Pd@TiO_2) was suspended in 4 mL of Milli-Q water, 4 mL of EtOH (99%) and 10 mg of benzoin Irgacure-2959TM (I-2959). The slurry was subsequently irradiated for 5 hours under UVA at room temperature. The mixture was then centrifuged, wash with Milli-Q water 4 times, dried in a desiccator and kept under Ar atmosphere.

Calculation of metal NP's surface atoms

For a NP of radius **R**, we can calculate the total number of atoms –of atomic radius **r**– within the NP by equation (1):[3]

$$N = \left(\frac{R}{r}\right)^3 \tag{1}$$

We may also calculate the surface (S) area of a nanoparticle with the following equation:

$$S_{NP} = 4\pi R^2 \tag{2}$$

and the number of surface atoms, N_s, directly by dividing the surface area of the NP by the cross section of an individual atom, and then simplifying using the relationship in equation (1):

$$N_S = 4\pi R^2/\pi r^2 = 4N^{2/3} \tag{3}$$

From TEM imaging and ICP-OES analysis we can determine the particle size and the metal loading of the catalyst, and build Table S1.

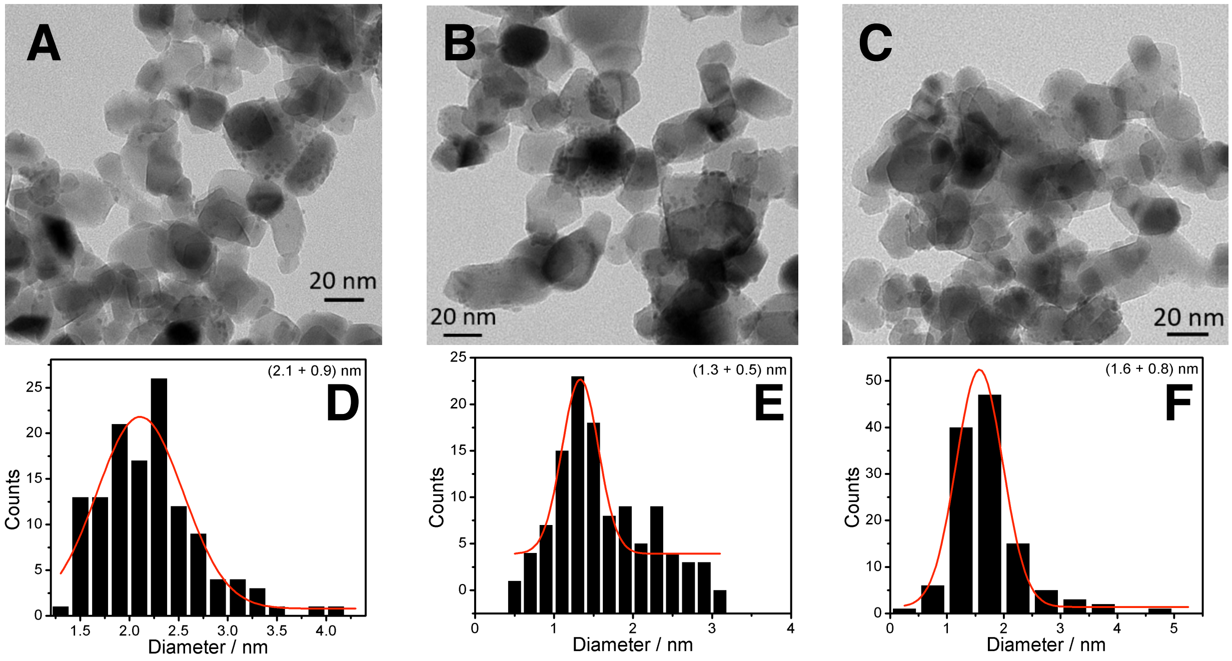

Figure S1. TEM images and PdNP size distribution for three different batches of Pd@TiO_2: (A/D) batch A, (B/E) batch B, and (C/F) batch C.

Table S1. Total number (N) of Pd atoms per NP and surface atoms (N_S) calculated using equations (1) and (3).

Batch	Pd (wt %)[a]	R (nm)[b]	r (nm)	N (per NP)	N_S (per NP)	Pd N_S (µmol/20mg)
A	2.3	1.05	0.137	450	235	2.3
B	2.7	0.65		107	90	4.3
C	3.4	0.80		199	136	4.4

[a] Metal loading determined by ICP-OES. [b] Size determined by TEM imaging.

Photochemical coupling of benzyl radicals

In a conventional reaction, 20 mg of catalyst were mixed together with 4 mL of solvent (toluene or *p*-xylene) and irradiated under UVA light (Figure S2) under Ar atmosphere and continuous stirring (Scheme S1 and Scheme S2). The coupling reaction must occur under inert atmosphere because the presence of O_2 results in the auto-oxidation of toluene, thus producing benzaldehyde (Figure S4).[4] Hence, no coupling products are detected when the reaction is run under air (Table 1 and Table S2). Furthermore, both solvents toluene and *p*-xylene were dried using molecular sieves to ensure there is no water present.

A few experiments were carried out using commercially available Au@TiO_2 to compare its performance with that of Pd@TiO_2. It soon became clear that Pd@TiO_2 was a much better performer as a catalyst for head-to-ring addition (Table 1 and Table S2).

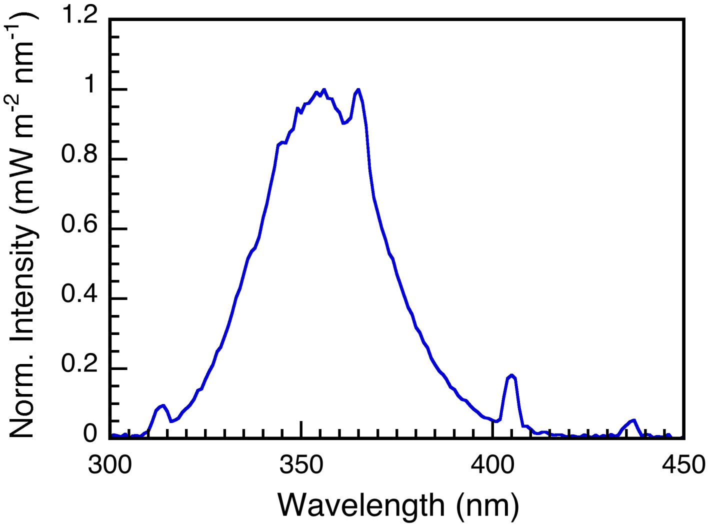

Figure S2. Emission spectrum of UVA lamps (λ ~355 nm) used in this work.

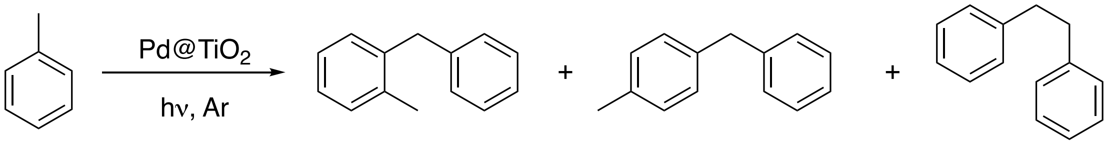

Scheme S1. Photochemical coupling of benzylic radicals derived from toluene.

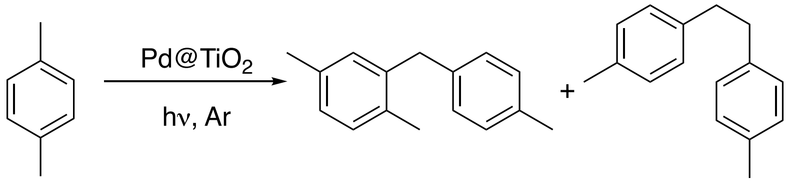

Scheme S2. Photochemical coupling of benzylic radicals derived from *p*-xylene.

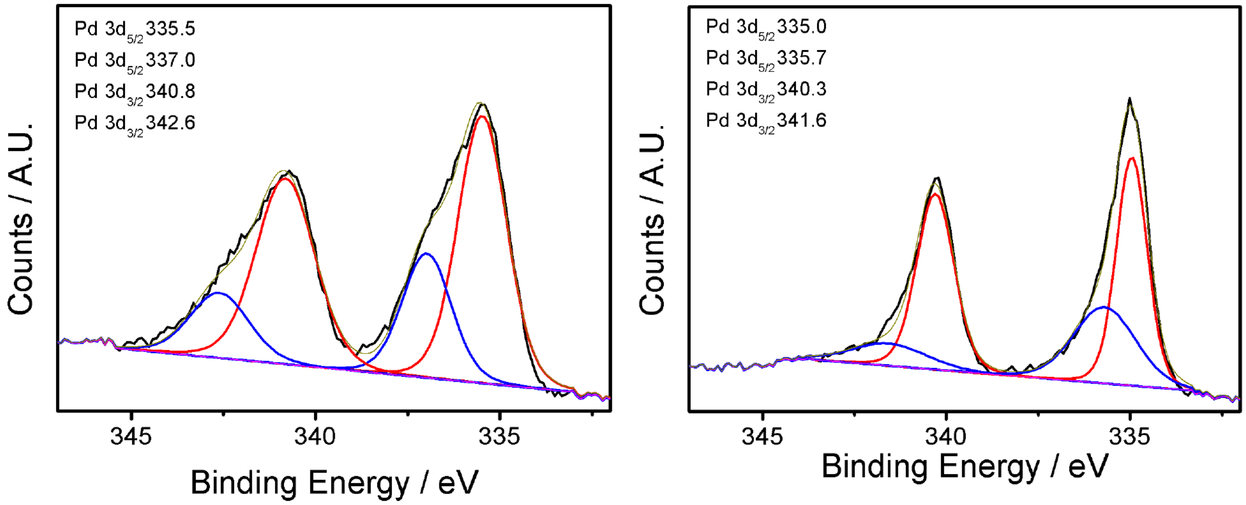

Figure S3. Pd 3d HR XPS spectra for (left) fresh catalyst and (right) reduced catalyst, showing the presence of more oxidised Pd species in the fresh catalyst.

Table S2. Fraction of **BB** (head-to-head coupling) and ***o*P/*p*P** (head-to-ring coupling) products for the reaction of toluene using different catalyst.[a]

Catalyst	Change in conditions	**BB**, %	***o*P**, %	***p*P**, %
TiO_2	none	97.7 ± 0.9	1.6 ± 0.9	0.8 ± 0.1
$Au@TiO_2$	none	88 ± 1	7.7 ± 0.4	3.8 ± 0.8
$Pd@TiO_2$	none	75 ± 1	13.2 ± 0.9	12.2 ± 0.6
$Pd@TiO_2$	under air	------	------	------
$Pd@TiO_2$	reduced catalyst	70 ± 2	14.7 ± 0.6	16 ± 2
None		------	------	------

[a] Reaction conditions: 4 mL of dried toluene and 20 mg of catalyst under Ar atmosphere and UVA irradiation for 20 h.

Table S3. Fraction of **BB** (head-to-head coupling) and ***oP*** (head-to-ring coupling) products for the reaction of *p*-xylene using different catalyst.[a]

Catalyst	**BB** (head-to-head), %	***oP*** (head-to-ring), %
TiO_2	98 ± 1	2 ± 1
$Au@TiO_2$	96.1 ± 0.3	3.9 ± 0.2
$Pd@TiO_2$	77 ± 2	23 ± 2

[a] Reaction conditions: 4 mL of dried *p*-xylene and 20 mg of catalyst under Ar atmosphere and UVA irradiation for 20 h.

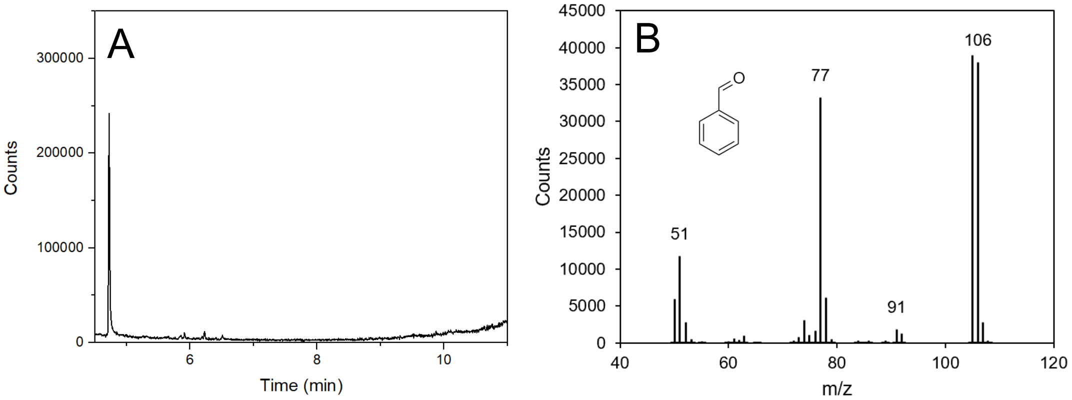

Figure S4. (A) Gas chromatograph of the photochemical reaction of toluene with Pd@TiO$_2$ under air, irradiated under UVA light for 1 hour. (B) MS spectrum of the product (benzaldehyde).

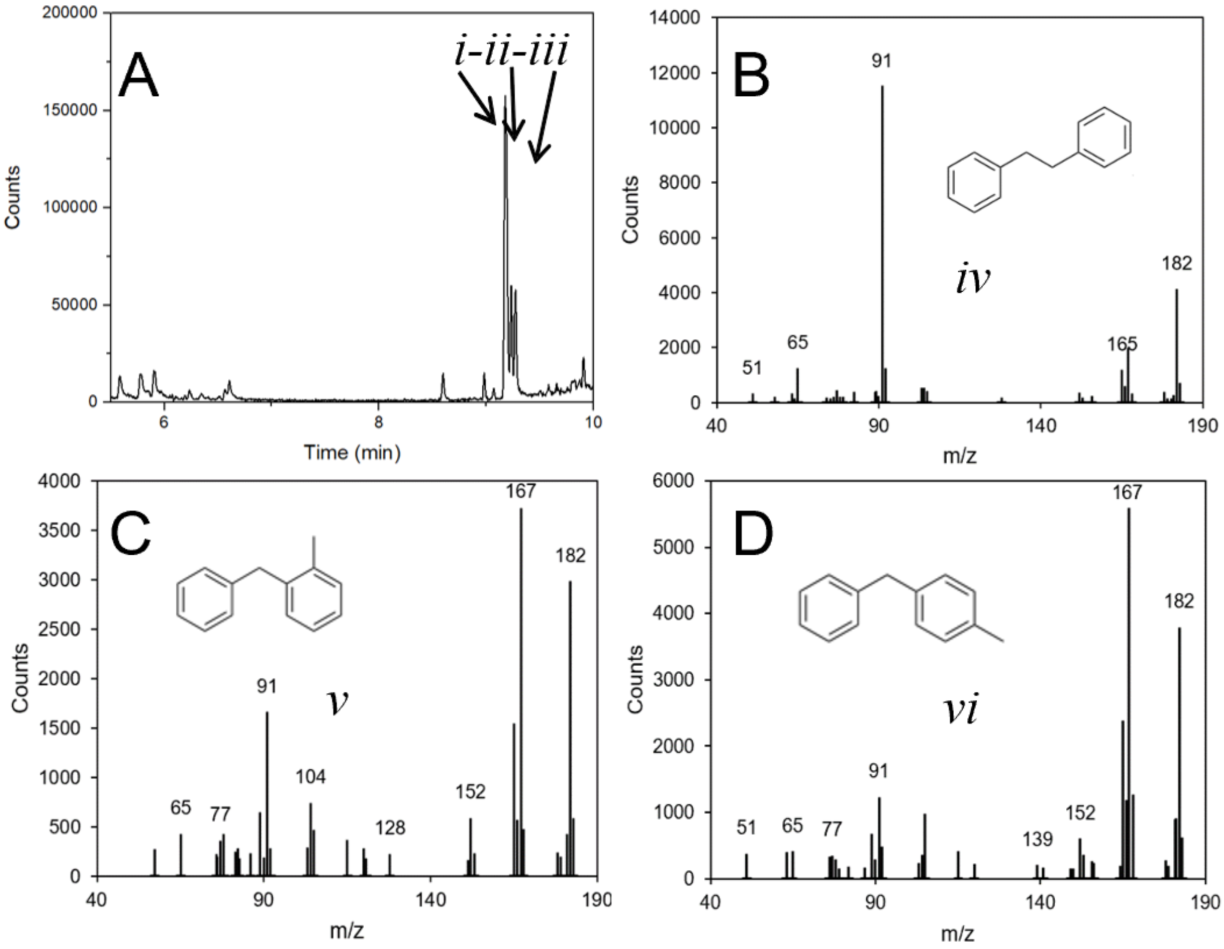

Figure S5. (A) Gas chromatograph of the photochemical reaction of toluene (dried) with Pd@TiO$_2$ under Ar, irradiated under UVA light for 20 hours. (B-D) MS spectra of the products.

Photolysis of dibenzyl ketone (DBK)

The photochemical coupling of benzyl radicals formed from dibenzyl ketone was evaluated as follows: a solution of dibenzyl ketone (1 mM) in 4 mL of toluene was irradiated under UVB (λ_{max}: 313 nm) light for 1 hour, under Ar and constant stirring. The product was characterized by GC-MS. The experiments were run in duplicates (Scheme 1 and Figure S6) and furnished the 1,2-diphenyl ethane as the only product. Therefore, under UVB light irradiation, dibenzyl ketone is decomposed into benzyl radicals and carbon monoxide, generating only the head-head product (**BB**). We note that under these conditions no head-to-ring coupling products were detected. This finding suggests that the head-to-ring coupling is only favoured in the presence of the heterogeneous Pd@TiO_2 catalyst.

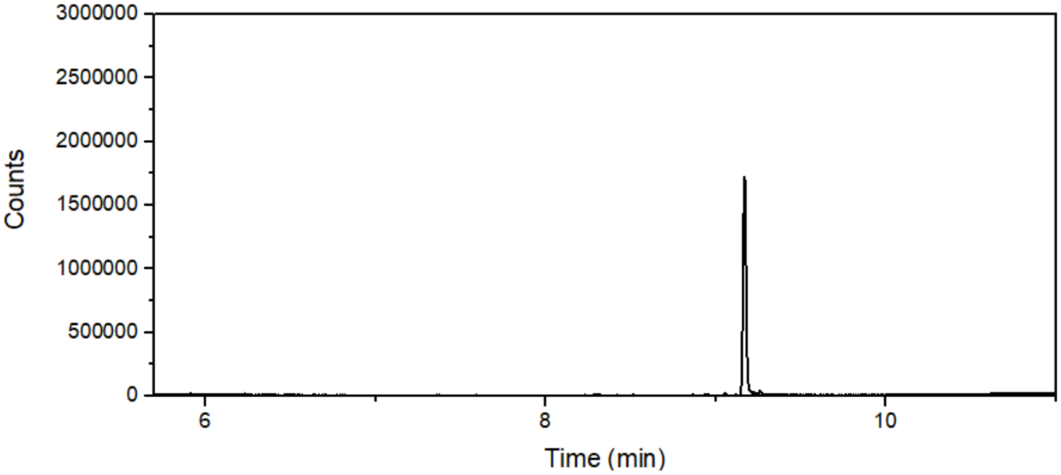

Figure S6. Gas chromatograph of the photochemical reaction of dibenzyl ketone showing only one product: diphenyl ethane.

Table S4. Fraction of ***oP*** product (head-to-ring coupling) for the reaction of *p*-xylene using different light intensities and different catalyst batches.

Intensity (W m^{-2})	Pd@TiO_2 (A)	Pd@TiO_2 (B)	Pd@TiO_2 (C)
17.672	21 ± 1	29 ± 3	36 ± 3
11.155	21.8 ± 0.2	40 ± 3	50 ± 2
7.801	31 ± 3	45 ± 4	58 ± 2
4.719	44 ± 3	57 ± 2	67 ± 8
3.896	-	93 ± 2	98 ± 1

Reaction conditions: 4 mL of dried *p*-xylene with 20 mg of catalyst under Ar atmosphere and UVA irradiation for 1h.

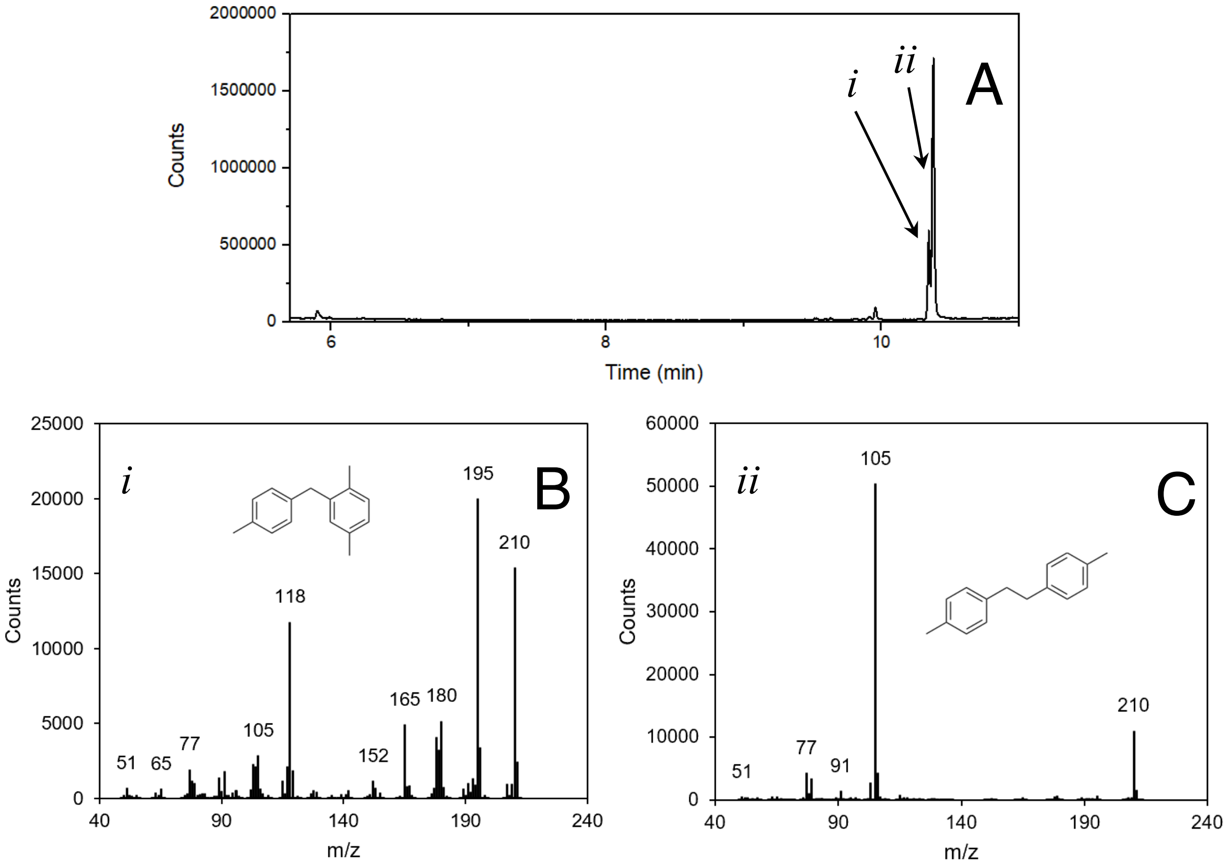

Figure S7. (A) Gas chromatograph of the photochemical reaction of p-xylene with Pd@TiO_2 under Ar, irradiated using 2 UVA lamps for 1 h. (B-C) The MS spectra of the products are shown.

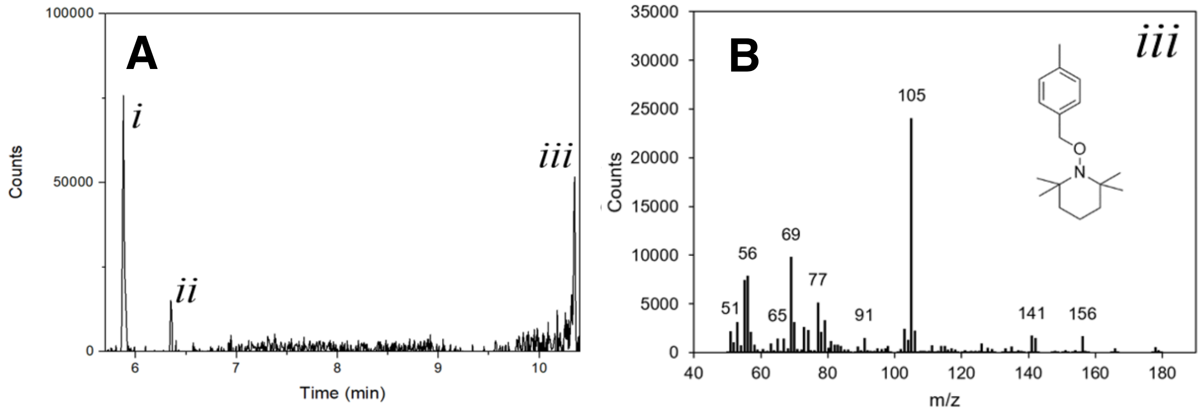

Figure S8. (A) Gas chromatograph of the photochemical reaction of *p*-xylene with Pd@TiO$_2$ in the presence of 25 mM of TEMPO under Ar atmosphere and UVA irradiation for 1.5 h: (i) 4-methylbenzaldehyde, (ii) TEMPO, (iii) radical-TEMPO adduct. (B) The MS spectrum of the radical-TEMPO adduct.

Computational analysis

Computational details

The spin-polarised DFT calculations for studying the interaction between the benzyl radical and metal clusters (Pd_{225} and Au_{225}) were carried out using Quantum ESPRESSO package.[5] Geometry optimization was performed throughout the generalized-gradient approximation (GGA) of Perdew–Burke–Ernzerhof (PBE) using projector augmented wave (PAW) method for describing the interaction between the atomic cores and valence electrons,[6-8] and including Grimme dispersion correction (DFT-D3). [9] All the atomic positions were allowed to relax during structural optimization until residual forces were smaller than 0.05 eV/Å. The Pd_{225} and Au_{225} clusters were placed in a box of 25 Å × 25 Å × 25 Å, in order to treat the nanoparticle as an isolated system. During the optimization of the complexes only the adsorbate and the uppermost two metal layers of the Pd clusters facet were allowed to relax. The adsorption energies were calculated by the following formula: $E_{ads} = E_{ab} - E_a - E_b$, where E_{ab} is the energy of the optimized complex (adsorbate + Pd_{225}/Au_{225} clusters), E_a is the energy of the optimized adsorbate and E_b is the energy of optimized Pd_{225}/Au_{225} clusters.

DFT calculations for analyzing the interaction between benzyl radical and a single atom of Pd electron were performed using Gaussian 09.[10] The geometry optimization were performed at BP86 functional[11] with Grimme's dispersion correction[9] using Def2-TZVP basis set.[12]

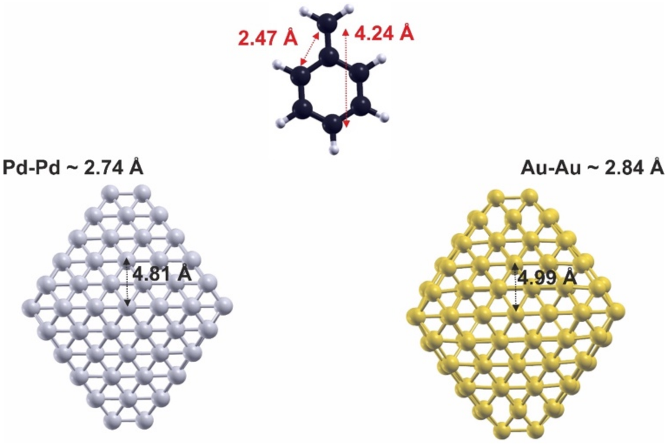

Figure S9. Optimized structures of benzyl radical (top), Pd_{225} (bottom left) and Au_{225} clusters (bottom right).

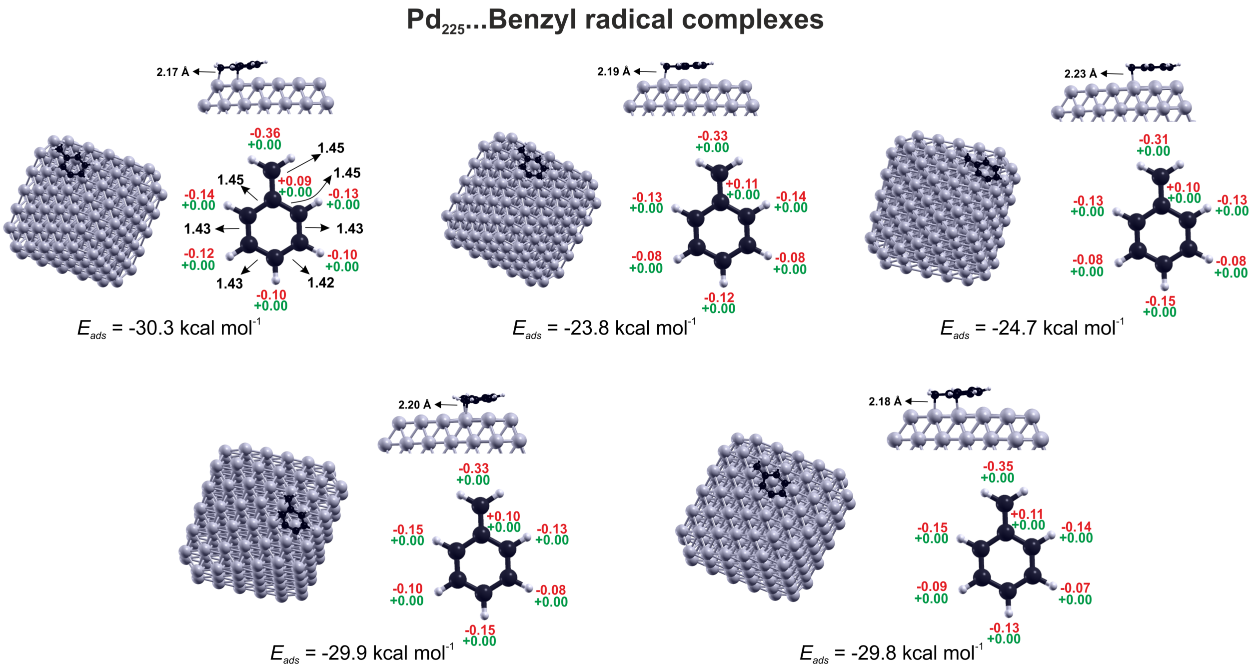

Figure S10. Optimized structures of the complexes between benzyl radical and Pd_{225} clusters showing the partial charge (in red), the spin polarization (in green) and the C-Pd bond length (in black).

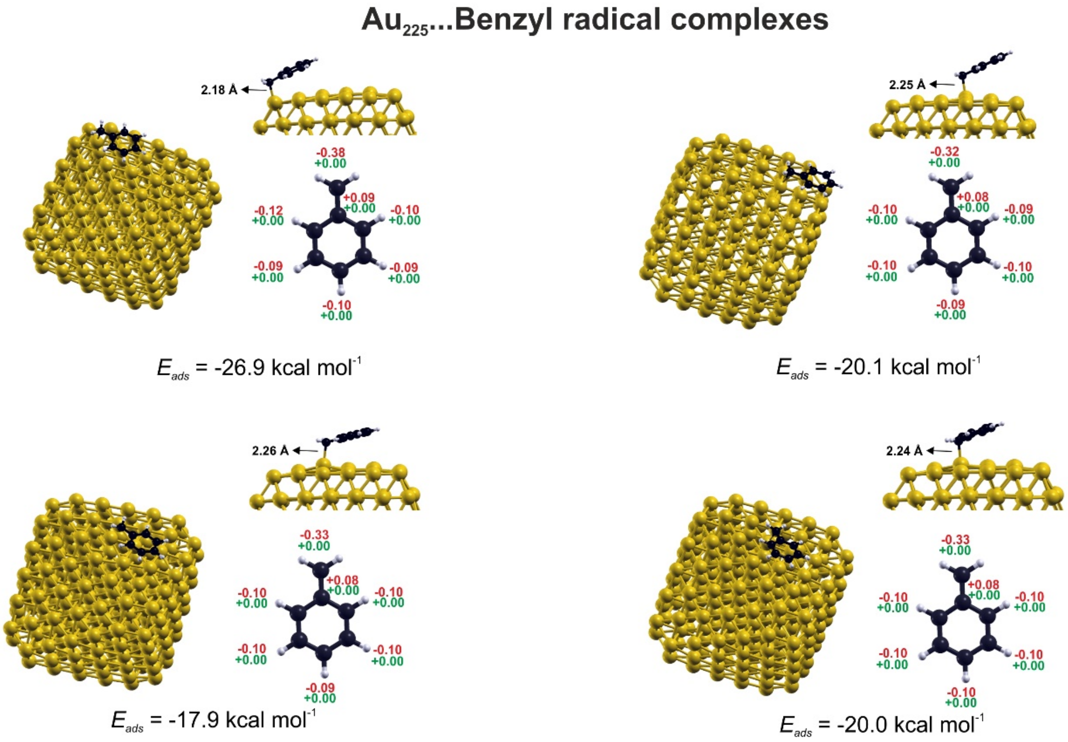

Figure S11. Optimized structures of the complexes between benzyl radical and Au_{225} clusters showing the partial charge (in red) and the spin polarization (in green) the C-Au bond length (in black).

References

1. Marina, N.; Lanterna, A. E.; Scaiano, J. C., Expanding the color space in the two-color heterogeneous photocatalysis of Ullmann C–C coupling reactions *ACS Catal.* **2018,** 8, 7593.

2. Elhage, A.; Lanterna, A. E.; Scaiano, J. C., Light-induced sonogashira C-C coupling under mild conditions using supported palladium nanoparticles *ACS Sust. Chem. Eng.* **2018,** 6, 1717.

3. Johnston, R., *Atomic and molecular clusters*. CRC Press: London, 2002.

4. Hermans, I.; Peeters, J.; Vereecken, L.; Jacobs, P. A., Mechanism of thermal toluene autoxidation *ChemPhysChem* **2007,** 8, 2678.

5. Giannozzi, P.; Baroni, S.; Bonini, N.; Calandra, M.; Car, R.; Cavazzoni, C.; Ceresoli, D.; Chiarotti, G. L.; Cococcioni, M.; Dabo, I.; Dal Corso, A.; de Gironcoli, S.; Fabris, S.; Fratesi, G.; Gebauer, R.; Gerstmann, U.; Gougoussis, C.; Kokalj, A.; Lazzeri, M.; Martin-Samos, L.; Marzari, N.; Mauri, F.; Mazzarello, R.; Paolini, S.; Pasquarello, A.; Paulatto, L.; Sbraccia, C.; Scandolo, S.; Sclauzero, G.; Seitsonen, A. P.; Smogunov, A.; Umari, P.; Wentzcovitch, R. M., Quantum espresso: A modular and open-source software project for quantum simulations of materials *J. Phys.: Condens. Matter* **2009,** 21.

6. Perdew, J. P.; Burke, K.; Ernzerhof, M., Generalized gradient approximation made simple *Phys. Rev. Lett.* **1996,** 77, 3865.

7. Kresse, G.; Joubert, D., From ultrasoft pseudopotentials to the projector augmented-wave method *Phys. Rev. B* **1999,** 59, 1758.

8. Blöchl, P. E., Projector augmented-wave method *Phys. Rev. B* **1994,** 50, 17953.

9. Grimme, S.; Antony, J.; Ehrlich, S.; Krieg, H., A consistent and accurate ab initio parametrization of density functional dispersion correction (DFT-d) for the 94 elements H-pu *J. Chem. Phys.* **2010,** 132.

10. Gaussian 09, Revision E.01, M. J. Frisch, G. W. Trucks, H. B. Schlegel, G. E. Scuseria, M. A. Robb, J. R. Cheeseman, G. Scalmani, V. Barone, B. Mennucci, G. A. Petersson, H. Nakatsuji, M. Caricato, X. Li, H. P. Hratchian, A. F. Izmaylov, J. Bloino, G. Zheng, J. L. Sonnenberg, M. Hada, M. Ehara, K. Toyota, R. Fukuda, J. Hasegawa, M. Ishida, T. Nakajima, Y. Honda, O. Kitao, H. Nakai, T. Vreven, J. A. Montgomery, Jr., J. E. Peralta, F. Ogliaro, M. Bearpark, J. J. Heyd, E. Brothers, K. N. Kudin, V. N. 295 Staroverov, R. Kobayashi, J. Normand, K. Raghavachari, A. Rendell, J. C. Burant, S. S. Iyengar, J. Tomasi, M. Cossi, N. Rega, J. M. Millam, M. Klene, J. E. Knox, J. B. Cross, V. Bakken, C. Adamo, J. Jaramillo, R. Gomperts, R. E. Stratmann, O. Yazyev, A. J. Austin, R. Cammi, C. Pomelli, J. W. Ochterski, R. L. Martin, K. Morokuma, V. G. Zakrzewski, G. A. Voth, P. Salvador, J. J. Dannenberg, S. Dapprich, A. D. Daniels, Ö. Farkas, J. B. Foresman, J. V. Ortiz, J. Cioslowski, and D. J. Fox, Gaussian, 300 Inc., Wallingford CT, 2009.

11. Becke, A. D., Density-functional exchange-energy approximation with correct asymptotic behavior *Phys. Rev. A* **1988,** 38, 3098.

12. Weigend, F.; Ahlrichs, R., Balanced basis sets of split valence, triple zeta valence and quadruple zeta valence quality for H to Rn: Design and assessment of accuracy *PCCP* **2005,** 7, 3297.